USAFA-DF+PA-278

Cadet Second Class Mike Grimmer

Lieutenant Colonel David Richie

Department of Astronautics

11 April, 2014

Control Strategies for Debris in Spacecraft Formation Flight

I.   Introduction

In the early days of mankind experimenting with manned objects in space, most scientists believed that collisions between spacecraft were of little concern. After all, the operating zone for satellites is far greater than previous endeavors, like airplanes or automobiles. However, in the modern era, with thousands of satellites, the orbital planes around Earth have become far more crowded than previously anticipated. In 2009, a Russian satellite by the name of Cosmos 2251 collided with an American Iridium spacecraft. Given that the immense speeds that satellites experience while on orbit, both spacecraft were destroyed beyond repair. Furthermore, in 2013, Russia's Ball Lens satellite collided with space junk debris left over from China's Fegyun spacecraft. China tried to destroy this satellite a few years prior, but the explosion caused a large debris cloud to form, which is what Ball Lens hit. Mankind must find ways to operate in this increasingly hostile environment, and thus a lot of research has been performed to optimize control strategies both to endure collisions and to avoid them. Concurrently, formation flying spacecraft have grown in popularity in the last decade because of operational and cost advantages. Some advantages include increased flexibility, lower cost, more versatility with launch vehicles, graceful degradation via distributed functionality, and better imaging resolution.

Approved 11 Apr 14, DFER
GPS,

Projects like MIT's SPHERES have developed test beds for formation flying spacecraft. They have been developed to aid the development of formation flying techniques. SPHERES consists of three autonomous satellite-like objects that can maneuver and rotate in all directions. Using multiple satellites with cameras can yield better coverage and resolution for ground-based targets.

The potential for formation flying spacecraft is vast and may define the nature of satellites in Earth's orbit for the future. With even more spacecraft orbiting Earth in an increasingly crowded area, control strategies regarding collisions are becoming critical for mission success. This paper will examine how multiple satellites can respond to oncoming disturbances and react in an appropriate manner to fulfill mission requirements in conjunction with spacecraft limitations.

II.   The Scenario

Two SPHERES-equivalent spacecraft are orbiting in a sun-synchronous orbit, which is defined as passing the same segment of the ground track at the same time of day. This orbit is useful for remote-sensing missions because the satellites will pass over the same locations on Earth with the same sun angle each time. In this scenario, the orbit is defined with an altitude of approximately 686 km above Earth's surface, an inclination of approximately 95 degrees, and an eccentricity of 0. Useful specifications for a SPHERES satellite is defined below in Table 1:

Table 1

SPHERES Specifications

Diameter	0.2 m
Mass	3.4 kg
Max Angular Acceleration	3.5 rad/s^2

Inertia	0.0136 kg m^2

The next question regards command configuration and dissemination. In a study performed by the NASA Goddard Space Flight Center, they determined that if a constellation has fewer than 16 satellites, it is less computationally burdensome and more efficient to have a master and slave configuration, as opposed to tracking a virtual center located in the middle of the constellation. This will provide more autonomy for the spacecraft and will provide conditions for the necessary corrective control commands. This will in turn reduce the ground support required.

In this mission, the two satellites will be in formation, side by side, in the aforementioned sun-synchronous orbit. The payload on board for each will be an imaging camera with CCD (charged-coupled device) capability. In very similar missions, such as BILSAT-1 and RADARSAT, performance specifications were defined like in Table 2:

Table 2

Mission Characteristics

Pointing Accuracy	0.2 degrees
Swath Width	~55 km
Gimbal Rate	9 deg/s
Average Wheel Speed	1000 rpm
Wheel torque	10 mNm (vacuum)

These performance specifications will drive the classical control performance parameters. The steady state error for each satellite will be 15% ±5% (in regards to how much they overlap). This is driven by the requirement that there must be at least 10% overlap in

images. Any more than 20% and the pictures will be redundant. Any less and the pictures would run the risk of not overlapping at all and not being synched. For a CCD of this nature, as defined by Sweedler et al in a 1991 Stanford study, the exposure time for the camera is 0.2 seconds, with a 4.8 recovery time. Thus, in order to not miss a picture, the settling time is 4.8 seconds. Lastly, the percent overshoot cannot exceed 70%. This is the most loosely defined performance specification, but having too much more overshoot than 70% might require too much torque from the reaction wheels to recover in time. The specifications are summarized in Table 3:

Table 3

Performance Specifications

Steady State Error	15%±5%
Settling Time	4.8 seconds
Percent Overshoot	70%

III. Collisions

In this sun-synchronous orbit, the speeds of the objects that are threats to the satellite constellation are relatively constant. They are defined as:

$$\sqrt{\frac{\mu}{R}} = \sqrt{\frac{398600.5 \ km^3/s^2}{(6378.137+686) \ km}} = 7.512 \ km/s \tag{1}$$

Since the diameter of each satellite is 0.2 meters, the moment arm is 0.1 meters in every direction. The momentum that the debris imparts on the satellite is dependent on the mass of the object. Note that the speed is doubled because it will be traveling in the opposite direction of the satellite in the same orbit, and a head-on collision is assumed.

$$F = mv = m\left(7.512\frac{km}{s} * 2\right) = m(15.024\frac{km}{s}) \tag{2}$$

The two major variables that decide whether the satellite will recover in time is the mass of the object and how far on the moment arm it hit. A wrench in the design is the consideration that the

debris might collide with the satellite in the middle of the recharge time for the camera, and not immediately after the exposure time. Thus, the satellite will be assumed to start the 5 second process (4.8 second recovery with a 0.2 second exposure) at the moment of impact. Otherwise, the specification regarding settling time could become arbitrary, as the disturbance torque could occur immediately before the exposure time.

The equations of motion regarding each satellite can be represented by a state-space model. The equations of motion for each direction are:

$$I_1 \dot{\omega}_1 = (I_2 - I_3)\omega_2\omega_3 - I_{s_1}\dot{\omega}_{s_1} + I_{s_2}\omega_{s_2}\omega_{s_3} - I_{s_3}\omega_{s_3}\omega_{s_2} + g_1 \tag{3}$$

$$I_2 \dot{\omega}_2 = (I_3 - I_1)\omega_1\omega_3 - I_{s_2}\dot{\omega}_{s_2} - I_{s_1}\omega_{s_1}\omega_{s_3} + I_{s_3}\omega_{s_3}\omega_{s_1} + g_2 \tag{4}$$

$$I_3 \dot{\omega}_3 = (I_1 - I_2)\omega_1\omega_2 - I_{s_3}\dot{\omega}_{s_3} + I_{s_1}\omega_{s_1}\omega_{s_2} - I_{s_2}\omega_{s_2}\omega_{s_1} + g_3 \tag{5}$$

s1, s2, and s3 refer to the principal directions of torque on the spacecraft and g refers to outside disturbance torques. In the form $\dot{\bar{x}} = A\bar{x} + B\bar{u}$, we can define the following:

$$\dot{\bar{x}} = \begin{bmatrix} \dot{\theta}_1 \\ \ddot{\theta}_1 \\ \dot{\theta}_2 \\ \ddot{\theta}_2 \\ \dot{\theta}_3 \\ \ddot{\theta}_3 \end{bmatrix} = \begin{bmatrix} 0 & 1 & 0 & 0 & 0 & 0 \\ 0 & 0 & 0 & \frac{-I_{s_3}\omega_{s_3}}{I_1} & 0 & \frac{I_{s_2}\omega_{s_2}}{I_1} \\ 0 & 0 & 0 & 1 & 1 & 1 \\ 0 & \frac{I_{s_2}\omega_{s_3}}{I_2} & 0 & 0 & 0 & \frac{-I_{s_1}\omega_{s_1}}{I_2} \\ 0 & 0 & 0 & 0 & 0 & 1 \\ 0 & \frac{-I_{s_2}\omega_{s_2}}{I_3} & 0 & \frac{I_{s_1}\omega_{s_1}}{I_3} & 0 & 0 \end{bmatrix} * \begin{bmatrix} x_1 \\ x_2 \\ x_3 \\ x_4 \\ x_5 \\ x_6 \end{bmatrix} + \begin{bmatrix} 0 & 0 & 0 \\ \frac{1}{I_1} & 0 & 0 \\ 0 & 0 & 0 \\ 0 & \frac{1}{I_2} & 0 \\ 0 & 0 & 0 \\ 0 & 0 & \frac{1}{I_3} \end{bmatrix} * \begin{bmatrix} g_1 \\ g_2 \\ g_3 \end{bmatrix} \tag{6}$$

This can be simplified further by the requirement that the satellites are spherical. Thus, all inertias are equal, and the A matrix becomes dependent on reaction wheel speed.

There is a certain torque value that causes the satellite to be unable to recover within the prescribed specifications. This applies to a certain relationship between the mass of the object and where it impacts on the moment arm. Assuming a worst case scenario in the case of the moment arm, the simulations will set the impact at 0.1 m – the tip of the satellite. Thus, the

ability to recover and meet the specifications will rely on the mass of the object, while simplifying criteria like density or elasticity.

Defining the initial conditions for each satellite is important in the analysis of adding disturbance torques. In this scenario, the pitch and yaw can be assumed to be 0 degrees. The roll angle is defined by the characteristics of the camera. Since these cameras are operating in the visible spectrum, they range from 0.4μm to 0.7μm. The equation regarding resolution is below:

$$Res = \frac{2.44 * \lambda * h}{D} \qquad (7)$$

However, since the resolution should ideally be the same and the aperture diameter of the camera is constant, the maximum allowable slant range (h) can be found using the following:

$$\lambda_1 h_1 = \lambda_2 h_2, h_2 = \frac{\lambda_1 h_1}{\lambda_2} = \frac{0.7\mu m * 686km}{0.4\mu m} = 1200.5 \ km \qquad (8)$$

This will in turn define the spacing of the satellites.

Figure 1: Spacecraft Geometry
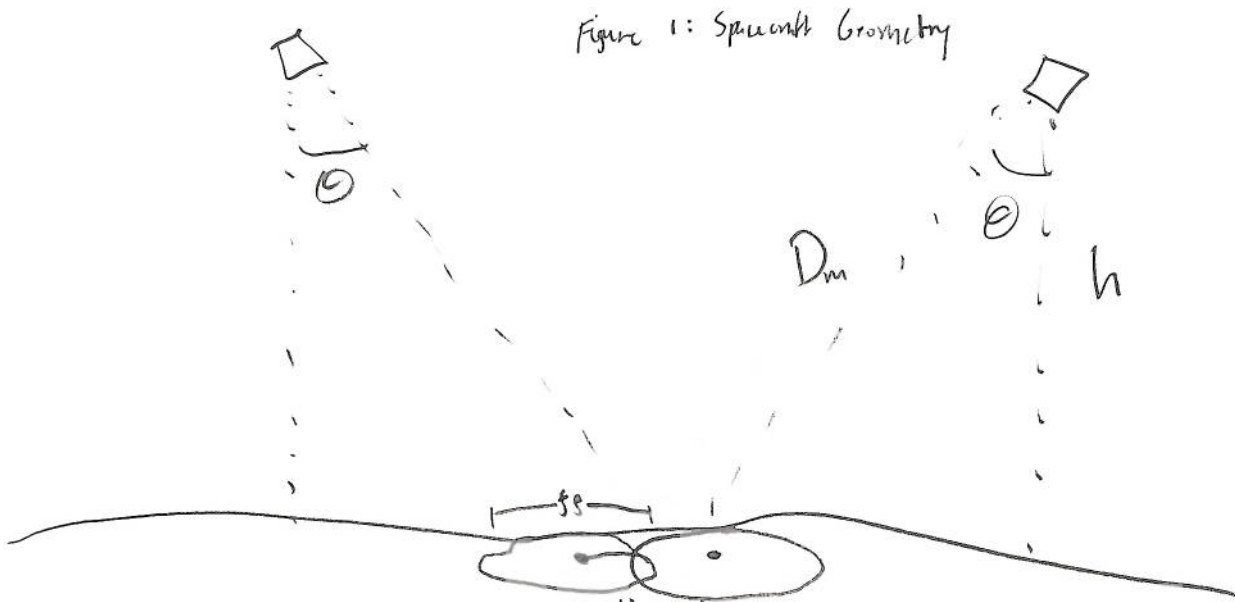
Furthermore, by nature of right triangles, the roll angle and separation between satellites in trail formation can be found:

$$2\sqrt{D_m^2 - h_2} - 11 = 2\sqrt{1200.5^2 - 686^2} - 11 = 1959.38 \ m \qquad (9)$$

$$\cos(\theta_1) = \frac{h}{D_m}, \theta_1 = 55.2 \text{ degrees} \tag{10}$$

The SIMULINK model regarding this scenario is expressed below in Figure 2. Note that the

block diagram has been simplified to only deal with the roll axis. Three degree axis control can

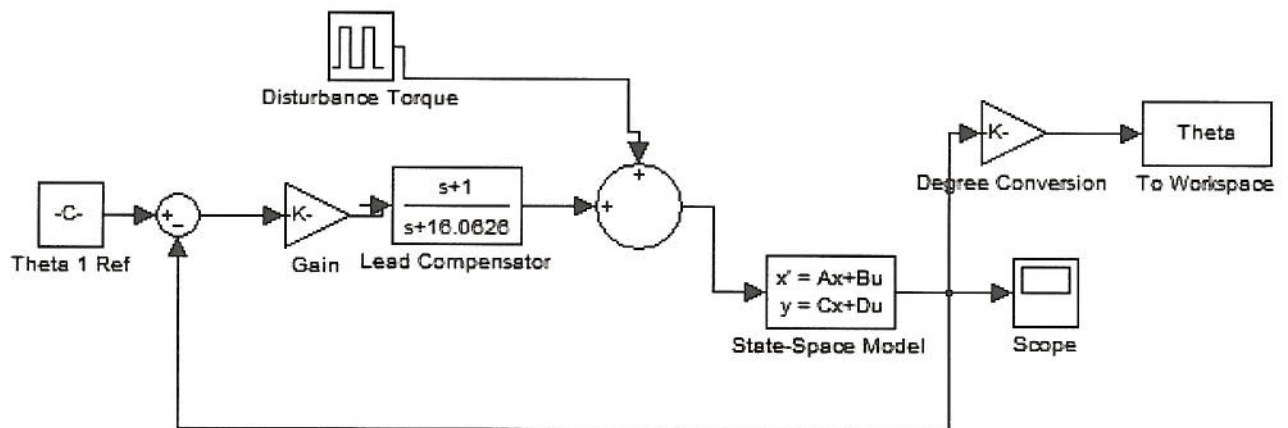be incorporated upon further research.

Figure 2: SIMULINK Block Diagram

The methodology for determining the lead compensator from the state-space model is

located in Appendix A. With zero disturbance torque and a θ_1 reference of 55.2 degrees, the

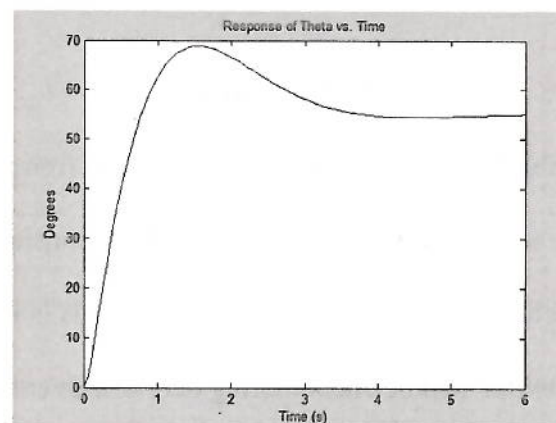response is simulated in Figure 3.

Figure 4: Zero Disturbance Torque Response

From this response, the settling time is 3.28 seconds and the percent overshoot is 24.62%, within the performance specifications previously defined. To push the design to the limits of adhering to the performance specifications, the torque of the disturbance increased until the performance specifications were broken. Note that the impulse time for momentum was approximated to be 0.1 seconds. After a series of trials, the maximum allowable torque was found to be 0.12 N*m. The response is shown below:
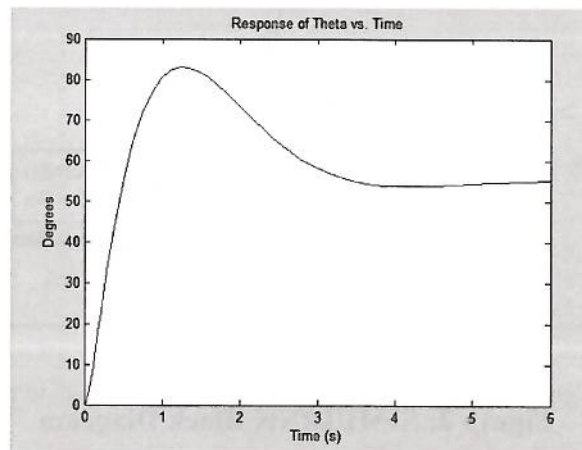

Figure 5: 0.12 N*m Torque Response

Under these conditions, the settling time was 4.8 seconds, and the percent overshoot was 61.52%.

IV. Conclusion

The maximum allowable torque in the worst case scenario (retrograde orbit hitting at the end of the moment arm at the normal angle) was 0.12 N*m. This translates to a mass of approximately 0.038 kg, which is roughly the size of a marble. This is indeed a very small piece of debris, but in orbit, the satellites will be encountering debris with extremely fast velocities, giving them a very substantial amount of momentum. There are a myriad of values for mass that

equal this disturbance torque accounting for different moment arms and incident angles. This is simply an analysis of the worst-case scenario for a disturbance torque.

This analysis demonstrates the necessity for being able to respond to disturbance torques with disturbance rejection. An analysis of passive disturbance rejection was considered above, but the spacecraft could be made more robust by making the disturbance active. One way of doing this is by spinning one of the other reaction wheels to harden the system to disturbances with precession.

V. Future Work

Although knowing control strategies to endure collisions is important, ideally, it would be better to avoid the collision altogether. Further work can be done in the context of SPHERES and applying and building off other research regarding sensors and the detection of oncoming disturbances. Also, in the scenario above, the satellites are assumed to survive the impact of the collision. In an operational context, this cannot be assumed. Depending on the material of the debris, the structural integrity of the satellite may be irrevocably compromised. A follow-up question may be regarding how much impact the satellites could endure before mission failure from structural damage. Lastly, after impact, the satellite will drift from its sun-synchronous course and fall out of formation with the other. Two burns will have to be performed on opposite sides of the orbit to correct for this perturbation (so as to avoid increasing eccentricity). Further work could be done to analyze how much ΔV is required to recover from such an incident.

The advent of formation flying has significant advantages in an operational capacity. With a robust disturbance rejection system, the constellation can react to endure or even avoid disturbances to complete the mission. In orbits that seem to be running out of space for satellites to maneuver, control strategies for disturbance rejection are vital for mission success. With

sophisticated systems, formation flying can become normal procedure and make space a more

prosperous and safe endeavor for all of mankind.

Appendix: Derivation of Lead Compensator

$$A = \begin{matrix} 0 & 1 & 0 & 0 & 0 & 0 \\ 0 & 0 & 0 & \frac{-I_{s3}\omega_{s3}}{I_1} & 0 & \frac{I_{s2}\omega_{s2}}{I_1} \\ 0 & 0 & 0 & 1 & 1 & 1 \\ 0 & \frac{I_{s2}\omega_{s3}}{I_2} & 0 & 0 & 0 & \frac{-I_{s1}\omega_{s1}}{I_2} \\ 0 & 0 & 0 & 0 & 0 & 1 \\ 0 & \frac{-I_{s2}\omega_{s2}}{I_3} & 0 & \frac{I_{s1}\omega_{s1}}{I_3} & 0 & 0 \end{matrix} \qquad (11)$$

$$B = \begin{matrix} 0 & 0 & 0 \\ \frac{1}{I_1} & 0 & 0 \\ 0 & 0 & 0 \\ 0 & \frac{1}{I_2} & 0 \\ 0 & 0 & 0 \\ 0 & 0 & \frac{1}{I_3} \end{matrix} \qquad (12)$$

$C = 1\ 0\ 0\ 0\ 0\ 0$ (since only θ_1 is being considered) (13)

$D = 0\ 0\ 0$ \qquad\qquad (14)

From classical control theory:

$$TF = C(sI - A)^{-1}B \qquad (15)$$

Using MATLAB:

[n,d] = ss2tf(A,B,C,D,1)

This function yields the plant transfer function:

$$Gp = \frac{73.5294s^2 + 1.8124}{s^4 + 0.0739s^2} \qquad (16)$$

Using the MATLAB code rlspecs.m, the Root Locus can be constructed with the performance specs superimposed on it:
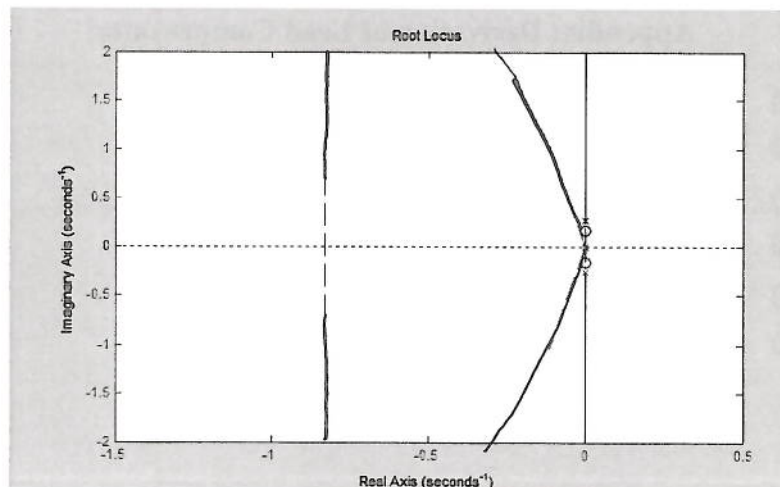
Figure 6: Root Locus of Plant

There is some discretion in choosing an operating point. It is even more important to give the

design more of a margin of failure, as the superposition of performance specifications on the

Root Locus are rules of thumb for second order systems, not a fourth order system. Giving the

design some margin for error while still in the realm of possibility, the operating point

s = -1+1.1j. Using the drop-down method, a lead compensator can be developed.

The phase of the plant was found to be 94.1768 degrees, so the compensator must be

~85.82 degrees to be located on the Root Locus. The zero is defined at s=-1, so, by geometry, the

pole must be at s=-16.0626, demonstrated by the following figure:
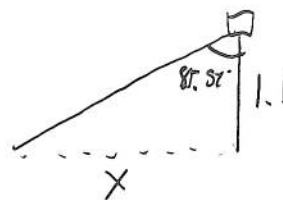

Figure 7: Geometry for Determining lead Compensator

To determine the magnitude of the lead compensator, the magnitude of the plant with this extra

pole and zero must be investigated. Determining the magnitude through MATLAB at the

operating point, the gain is 2.427. In order for the overall gain to be 1 and have the compensator

be included in the Root Locus, the compensator gain must be 1/2.427 or 0.412. Thus, the lead

compensator is established to be:

$$G_c = \frac{0.412(s+1)}{(s+16.0626)} \tag{17}$$

Works Cited

1. Miller, D, et al. "SPHERES: A Testbed For Long Duration Satellite Formation Flying In Micro-Gravity Conditions." *MIT Space Systems Lab*. N.p.. Web. 11 Apr 2014.

2. Bauer, Frank, et al. "Enabling Spacecraft Formation Flying through Spaceborne GPS and Enhanced Automation Technologies." . NASA Goddard Space Flight Center. Web. 11 Apr 2014.

3. Raney, Keith, et al. "RADARSAT." *IEEE*. 79. (1991): n. page. Print.

4. Gomes, Luis, et al. "BILSAT: Advancing Smallsat Capabilities." *DigitalCommons*. University of Surrey. Web. 11 Apr 2014.

5. Sweedler, J.V., et al. "Fluorescence Detection in Capillary Zone Electrophoresis Using a Charge-Coupled Device with Time-Delayed Integration."*Analytical Chemistry*. 63. (1991): n. page. Print.